THE ASTROPHYSICAL JOURNAL SUPPLEMENT SERIES, 77:59–66, 1991 September

A CATALOG OF BRIGHT-RIMMED CLOUDS WITH *IRAS* POINT SOURCES: CANDIDATES FOR STAR FORMATION BY RADIATION-DRIVEN IMPLOSION. I. THE NORTHERN HEMISPHERE

KOJI SUGITANI[1]
I. Physikalisches Institut, Universität zu Köln, Zülpicher Strasse 77, 5000 Köln 41, Germany
YASUO FUKUI
Department of Astrophysics, Nagoya University, Chikusa-ku, Nagoya 464-01, Japan
AND
KATSUO OGURA
Kokugakuin University, Higashi, Shibuya-ku, Tokyo 150, Japan
Received 1990 July 23; accepted 1991 January 22

ABSTRACT

Forty-four bright-rimmed clouds associated with *IRAS* sources have been selected from the Palomar Sky Survey prints. They are good candidates for the sites of star formation induced by radiation-driven implosions; three well-established cases of radiation-driven implosions in bright-rimmed globules have been reported elsewhere (see work by Sugitani et al.). Nine of the bright-rimmed clouds are known to be associated with molecular outflows and two (including one with an outflow) with HH objects. Most of their sizes are $\lesssim 1$ pc, similar to those of Bok globules. The luminosities of the associated *IRAS* sources are relatively large, $\sim 10-10^4\ L_\odot$, compared to those of the *IRAS* sources associated with dark globules or dense cores in dark cloud complexes. *IRAS* luminosity to cloud mass ratios are significantly greater than those in dark globules or in dense cores of dark cloud complexes.

Subject headings: infrared: sources — nebulae: H II regions — stars: formation

1. INTRODUCTION

Bright-rimmed clouds associated with old H II regions have long been suspected to be potential sites for star formation due to the compression by ionization-shock fronts. Reipurth (1983) produced evidence for star formation in some of the bright-rimmed cometary globules in the Gum Nebula, and he suggested the possibility of low-mass star formation in these globules due to UV radiation.

The *IRAS* Point Source Catalog has revealed a number of stellar objects which probably are younger than pre–main sequence stars (e.g., Beichman et al. 1986) and which serve as candidates to study very early stages of star formation. Reipurth & Gee (1986) and King (1987) have reported *IRAS* point sources embedded in bright-rimmed globules.

IRAS point sources associated with molecular outflows are considered to be the youngest solar-type stellar objects with ages of $\lesssim 10^5$ yr as shown by the Nagoya CO survey (Fukui et al. 1986, 1989; Fukui 1989). Molecular outflows associated with luminous *IRAS* sources ($L \sim 10-10^3\ L_\odot$) have so far been found in three bright-rimmed globules, Ori I-2, IC 1396-north, and L1206 (Sugitani et al. 1989). Velocity fields of ^{13}CO or C^{18}O and time scales of star formation strongly suggest induced star formation by radiation-driven implosions in these three globules. Similar examples were also reported in two bright-rimmed cometary globules, ESO 210-6A (HH 46/47) and CG 30 (HH 120), in the Gum Nebula region (Olberg, Reipurth, & Booth 1989), and in GN 21.38.9 in IC 1396 (Duvert et al. 1990).

Bright-rimmed globules are found in/around relatively old ($\tau \gtrsim 10^6$ yr) H II regions. Presumably, they were originally dense clumps in the parental molecular clouds and have emerged after the dispersion of the parental molecular gas due to UV radiation from OB stars. The physical conditions of such globules match well the theoretical implosion models of single massive stars, and it is expected that they are compressed effectively by radiation-driven implosions. The model of radiation-driven implosion has been studied theoretically as an effective process of star formation (Klein, Sandford, & Whitaker 1980; Sandford, Whitaker, & Klein 1982, 1984; LaRosa 1983; Bedijin & Tenorio-Tagle 1984; Klein, Sandford, & Whitaker 1985; Bertoldi 1989, Bertoldi & McKee 1990). If the molecular clouds are originally uniform, such implosion processes would not be expected; however, molecular clouds exhibit density inhomogeneities, i.e., clumps (e.g., Stutzki & Güsten 1990). The radiation-driven implosion processes are generally expected to take place in clumps associated with H II regions, which are effectively compressed due to accretion shocks of the focusing gas introduced by their curved surfaces (e.g., Bertoldi 1989). The density increase due to the compression is followed by rapid gas cooling and diffusion of the magnetic field (Elmegreen 1988). It is likely that stars form in the postshocked clouds. Therefore, we consider the radiation-driven implosion as an important process of star formation.

In the three bright-rimmed globules, Sugitani et al. (1989) found a much larger $L_{\rm IR}/M_{\rm cloud}$ ratio than for dark globules as one characteristic piece of evidence for the formation of more massive stars due to the radiation-driven implosions. However, the statistics are based on too small a number to establish a comprehensive understanding of star formation by such an implosion process. Star-formation frequency and efficiency and stellar mass function due to the implosions are still unknown. So, at present, improvement of the underlying observational statistics is particularly important.

[1] On leave from Nagoya City University.

In this paper, we present a catalog of bright-rimmed clouds associated with *IRAS* point sources in the northern hemisphere. Here, the bright-rimmed clouds include cometary globules and small clouds with curved bright rims. It is also our major aim to motivate further observations, at radio, infrared, and optical wavelengths, in order to reveal details and various physical aspects of star formation in shocked molecular gas.

2. THE SAMPLE

2.1. *Surveyed Regions*

Based on the Sharpless catalog (1959), a systematical search for bright-rimmed clouds in the northern hemisphere was made toward 65 H II regions with apparent extents of $\sim 60'$ or larger. We also searched other areas where prominent bright rims are seen. The extent of $\sim 60'$ corresponds to ~ 17 and ~ 35 pc at distances of 1 and 2 kpc from the sun, respectively. H II regions of these sizes with an expansion velocity of ~ 10 km s^{-1} should have ages of a few times 10^6 yr, which are presumably long enough for ionization-shock fronts to cause star formation in bright-rimmed clouds.

2.2. *Selection of Bright-rimmed Clouds with IRAS Sources*

The Palomar Sky Survey (PSS) red prints and the *IRAS* Point Source Catalog were used for the survey of the bright-rimmed clouds associated with *IRAS* sources. Here, we mainly searched small bright-rimmed clouds with sizes less than several arcminutes. Our sources were selected by using overlays showing *IRAS* point sources for the PSS prints. Only those clouds were included which have *IRAS* sources surrounded by curved bright rims. We excluded the bright-rimmed clouds which have *IRAS* sources located just on their bright rims, because such *IRAS* sources possibly are not stellar objects but emissions from dust knots. The accuracy of the *IRAS* identification should be better than one-fourth arcminute.

Some additional criteria were imposed on the properties of the *IRAS* flux qualities to exclude emission from diffuse dust. Only those *IRAS* sources were included which are detected at 25 μm as well as at least at one more band and which have point source correlation coefficients (CC) of F or better at 25 μm, where *IRAS* point sources have CC between 87%–100% which are encoded as $A = 100\%$, $B = 99\%, \ldots, N = 87\%$ (see the explanatory supplement of the *IRAS* catalog). The detection at 25 μm may help to exclude normal/field stars coinciding by chance with the bright-rimmed clouds. No criterion for confusion and cirrus flag was imposed, because *IRAS* sources toward H II regions generally have stronger contaminations from warm, extended emission than those in dark clouds not associated with H II regions.

We may have missed some bright-rimmed clouds with *IRAS* sources in our survey. In particular, H II regions with high surface brightness make such a survey difficult due to the saturation of the PSS prints. In fact, no bright-rimmed objects are detectable in S25 (M8) although many bright-rimmed globules are known to exist there (e.g., Osterbrock 1957). Also, rims of low brightness are not easy to detect. Third, due to the strong foreground emissions, we cannot pick up bright-rimmed clouds located on the far sides of the H II regions. Thus, our survey is limited to those objects only which are easy to detect. Nevertheless, we believe that this work bears source importance as a first systematical survey for bright-rimmed clouds with the aim to produce further evidence for star formation induced by the radiation-driven implosions.

3. RESULTS

We selected 44 bright-rimmed clouds associated with *IRAS* point sources in/around 18 H II regions. Their finding charts reproduced from the Palomar Sky Survey red prints are shown in Figure 1 (plates 1–7). The position of the *IRAS* point source is indicated by a couple of white or black dashes. Table 1 presents the H II regions where the bright-rimmed clouds associated with *IRAS* point sources were selected. The catalog of the bright-rimmed clouds is given in Table 2 and the properties of the associated *IRAS* sources are given in Table 3.

3.1. *Bright-rimmed Clouds*

The bright-rimmed clouds were classified into three types according to their rim morphology: (1) type A, moderately curved rim; (2) type B, tightly curved rim; and (3) type C, cometary rim. Their rim sizes, length (l), and width (w), are defined in Figure 2. Type A should have a length to width ratio, l/w, less than 0.5, and type B greater than 0.5. The range of their sizes is 0.2–3 pc and most of them are less than 1 pc (Table 2). The average lengths and widths of these three types of rims (except for the No. 36 cloud) are, respectively, as follows: type A, 0.39 pc and 1.0 pc (25); type B, 1.0 and 1.2 pc (15); and type C, 0.58 and 0.18 pc (3), where the values in the parentheses are the sample numbers.

TABLE 1

H II REGIONS WHERE BRIGHT-RIMMED CLOUDS WITH *IRAS* POINT SOURCES WERE SELECTED

H II Region	Size	d (kpc)	Ref. of d	Other Name
S49	90'	2.2	1	M16, Ser OB1
S117	240'	1.0	2	NGC7000
S131	170'	0.75	3	IC1396, Cep OB2
S142[a]	30'	2.4	4	NGC7380, Cep OB1
S145	90'	0.91	5	
S171	180'	0.85	6	NGC7822, Cep OB4
S185	120'	0.19	7	γ Cas
S190	150'	1.9	8	IC1805
S199	120'	1.9	8	IC1848
S236	55'	3.4	1	IC410, Aur OB2
S249	80'	1.6	9	
S264	390'	0.40	10	λ Ori
S273	250'	0.78	11	NGC2264, Mon OB1
S275	100'	1.42	12	Rostte Nebula, NGC2244 Mon OB2
S276	1200'	0.40	13	Barnard's Loop, L1634
S277	120'	0.40	14	IC434
S281	60'	0.46	15	Orion Nebula
S296	200'	1.15	16	CMa OB1

[a] Associated with prominent bright rims, although the size of H II region is <60'.

REFERENCES.—(1) Humphreys 1978; (2) Bally & Scoville 1980; (3) Matthews 1979; (4) Georgelin & Georgelin 1976; (5) Crampton & Fisher 1974; (6) MacConnell 1968; (7) Savage et al. 1977; (8) Ishida 1970; (9) Hardie, Seyfert, & Gulledge 1960; (10) Murdin & Penston 1977; (11) Turner 1976; (12) Ogura & Ishida 1981; (13) Reynolds & Ogden 1979; (14) Bok, Cordwell, & Cromwell 1971; (15) Blaauw 1964; (16) Claria 1974.

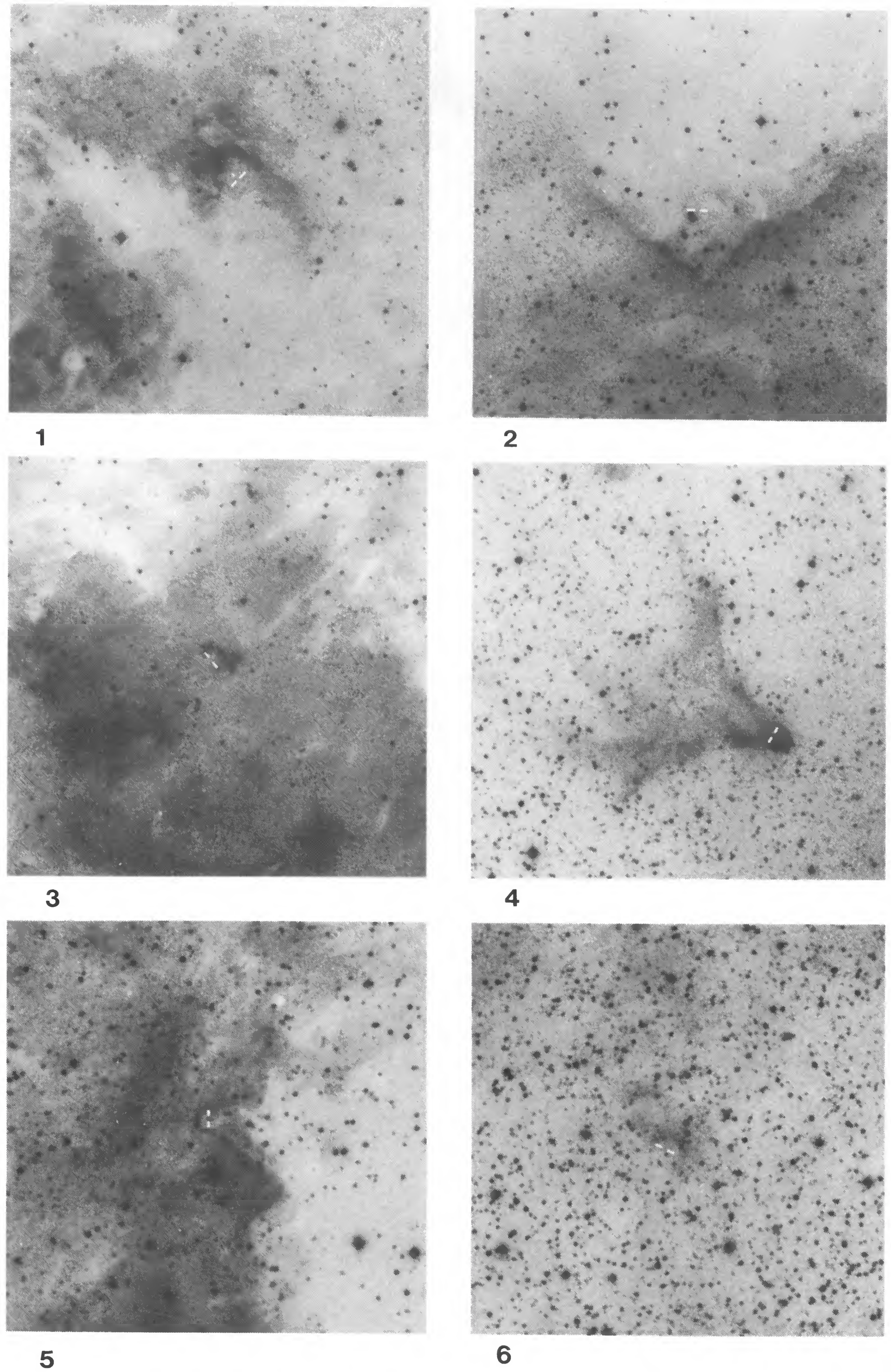

FIG. 1.—Finding charts for the bright-rimmed clouds. The charts are reproduced from the Palomar Sky Survey red prints. The position of the *IRAS* point source associated with the bright-rimmed cloud is indicated by a couple of white or black tips. 1 mm in the charts corresponds to 0'.28 except for the charts of panels 16–18, where 1 mm corresponds to 0'.56.

SUGITANI et al. (*see* 77, 60)

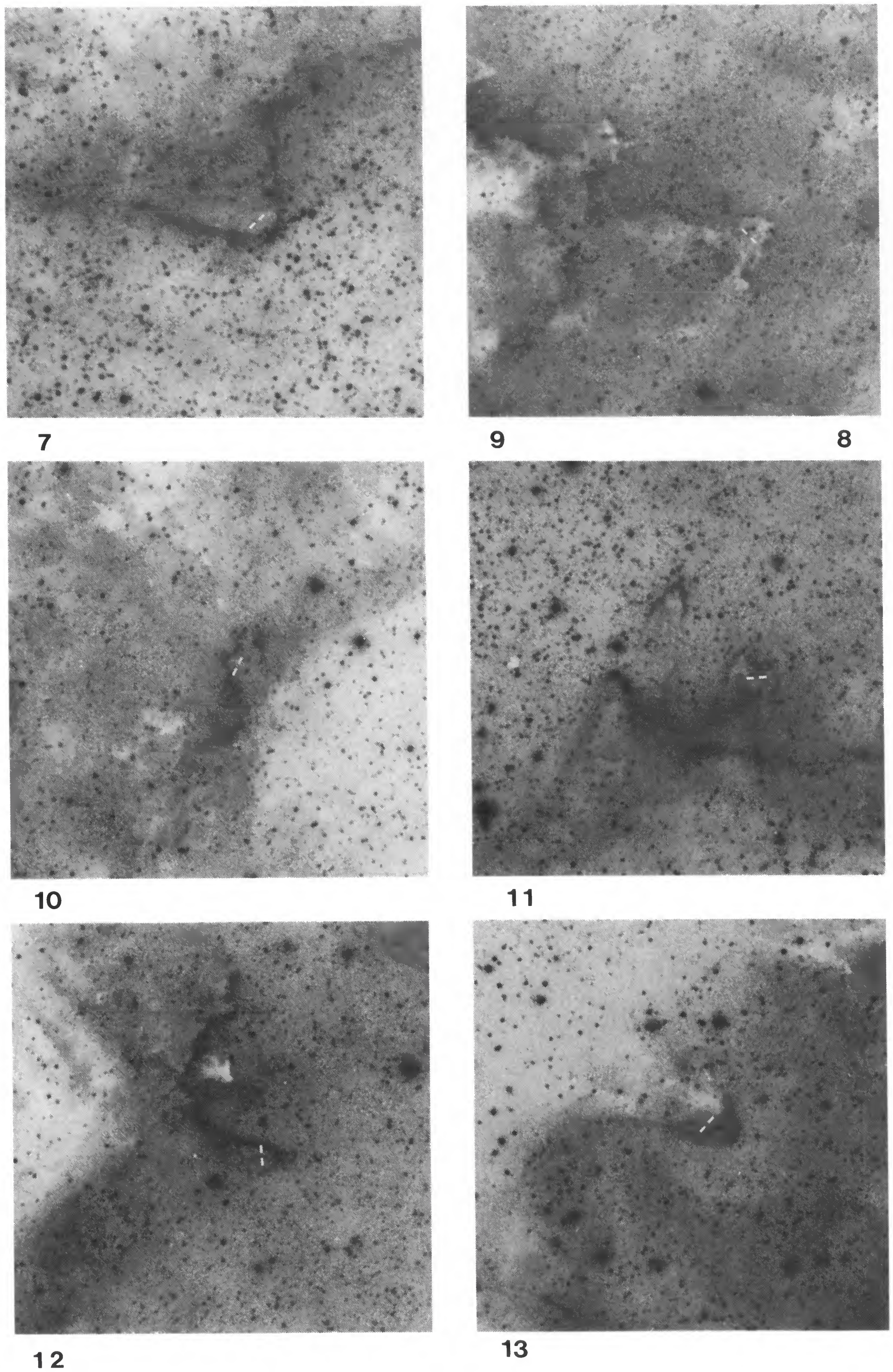

FIG. 1—*Continued*

SUGITANI et al. (*see* 77, 60)

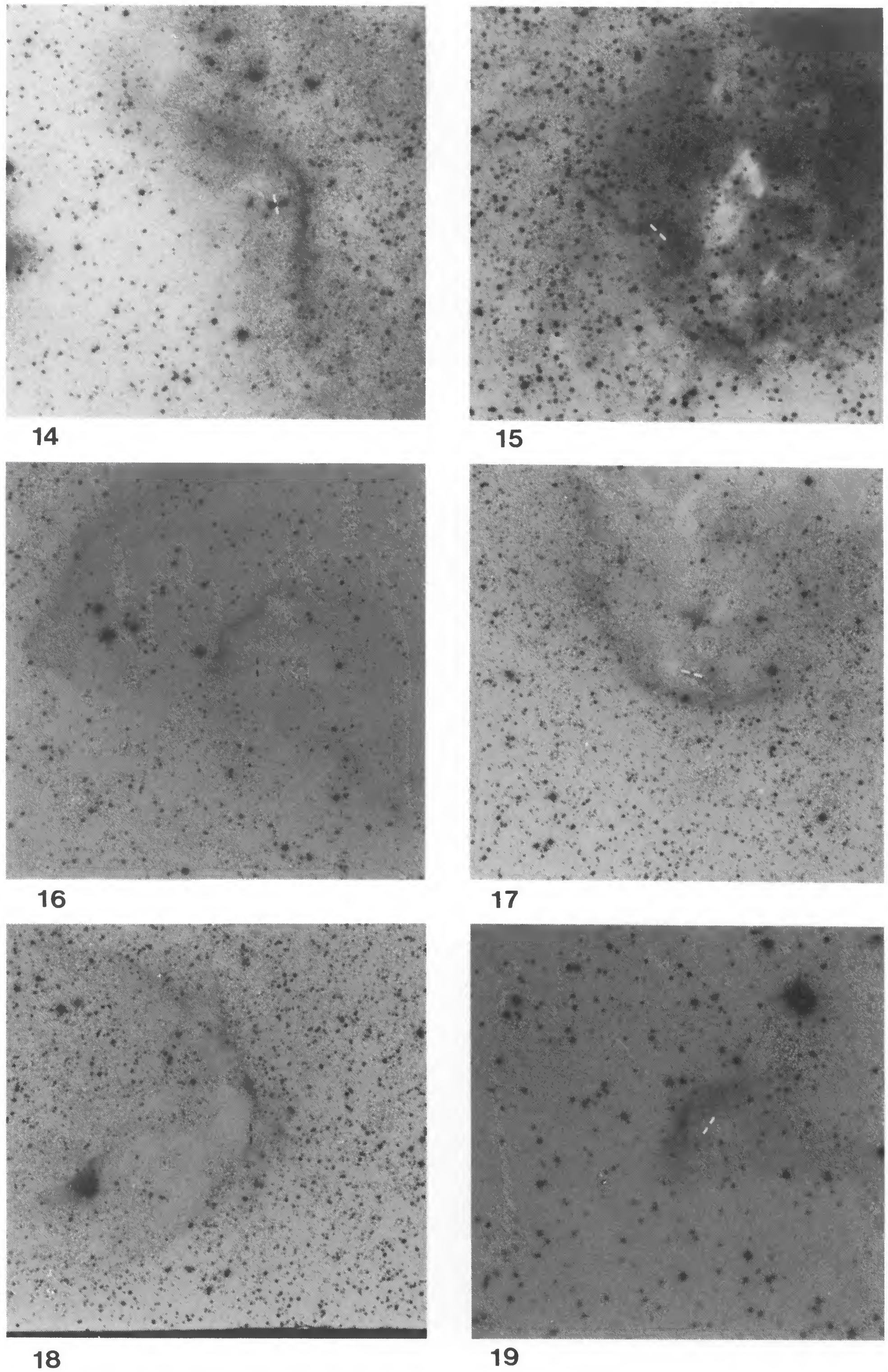

FIG. 1—*Continued*

SUGITANI et al. (*see* 77, 60)

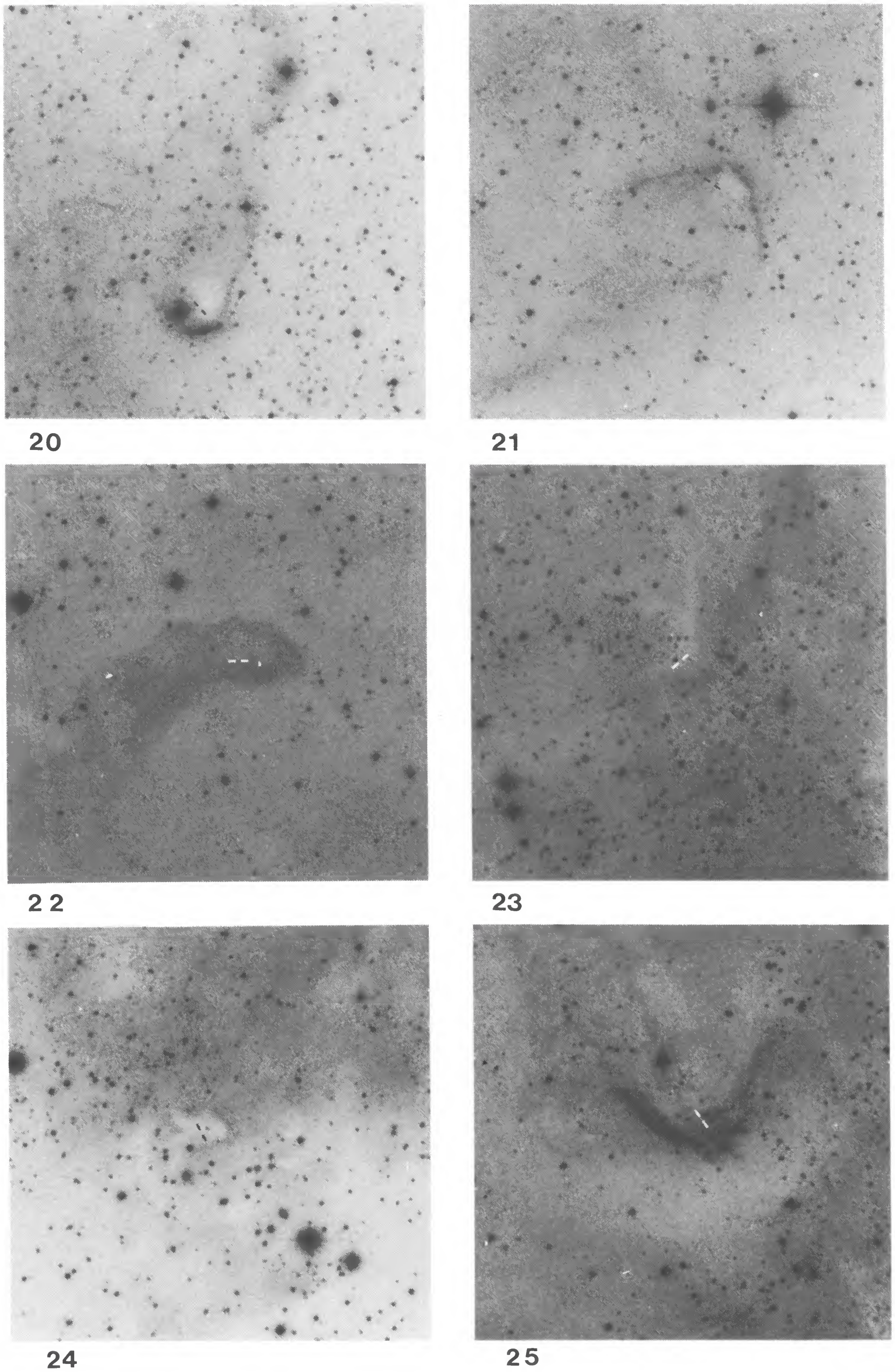

FIG. 1—*Continued*

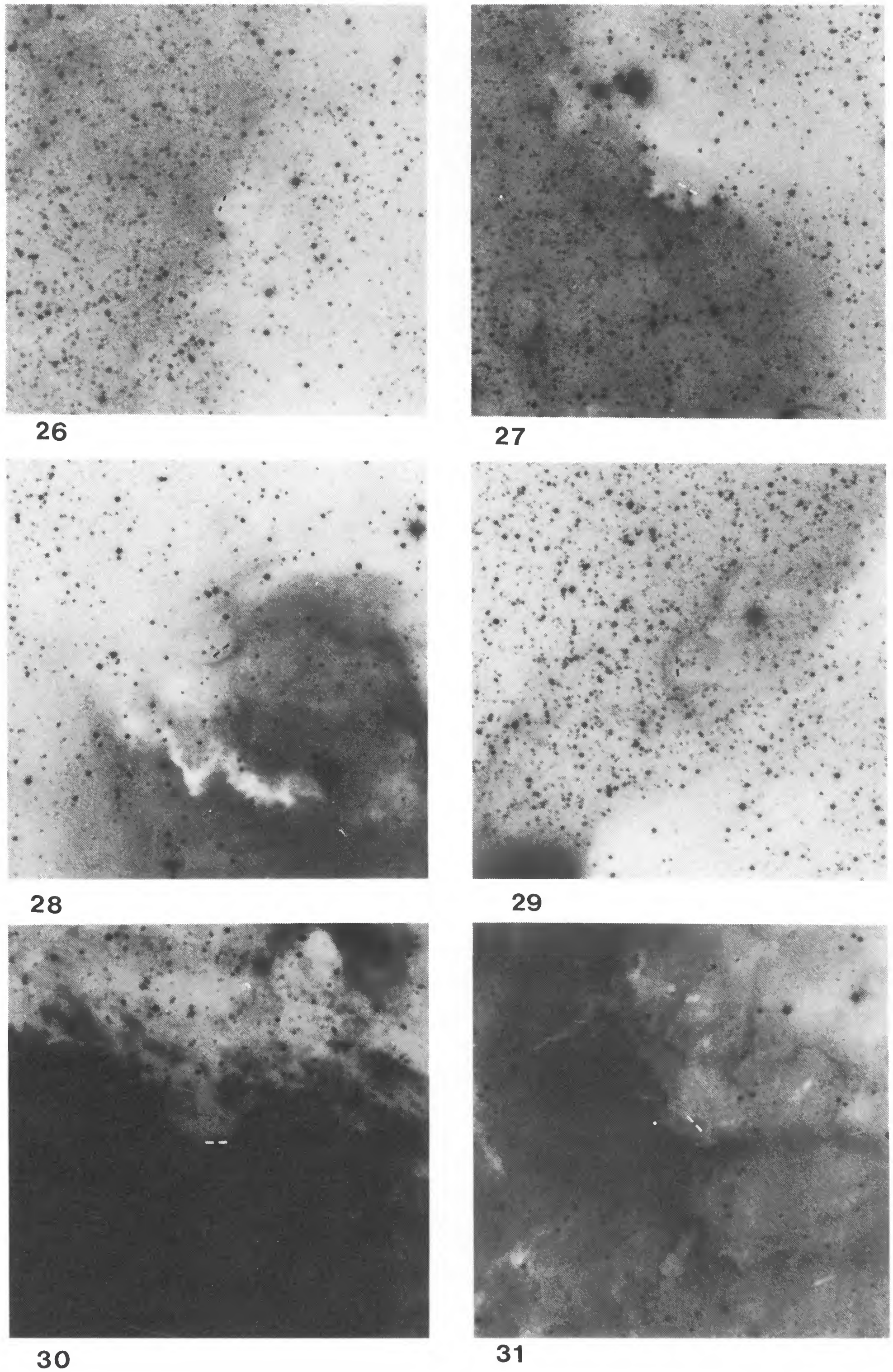

FIG. 1—*Continued*

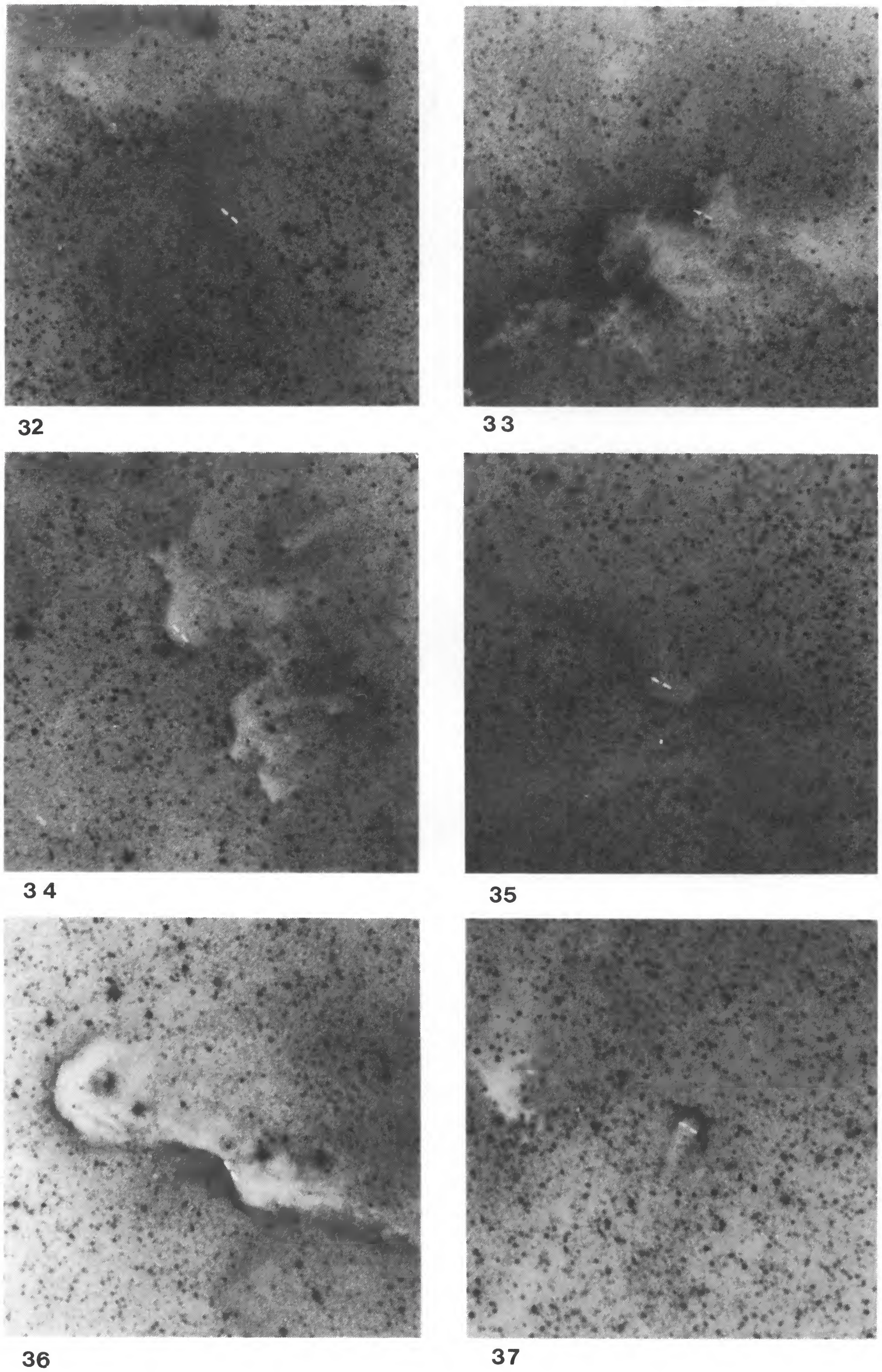

FIG. 1—*Continued*

SUGITANI et al. (*see* 77, 60)

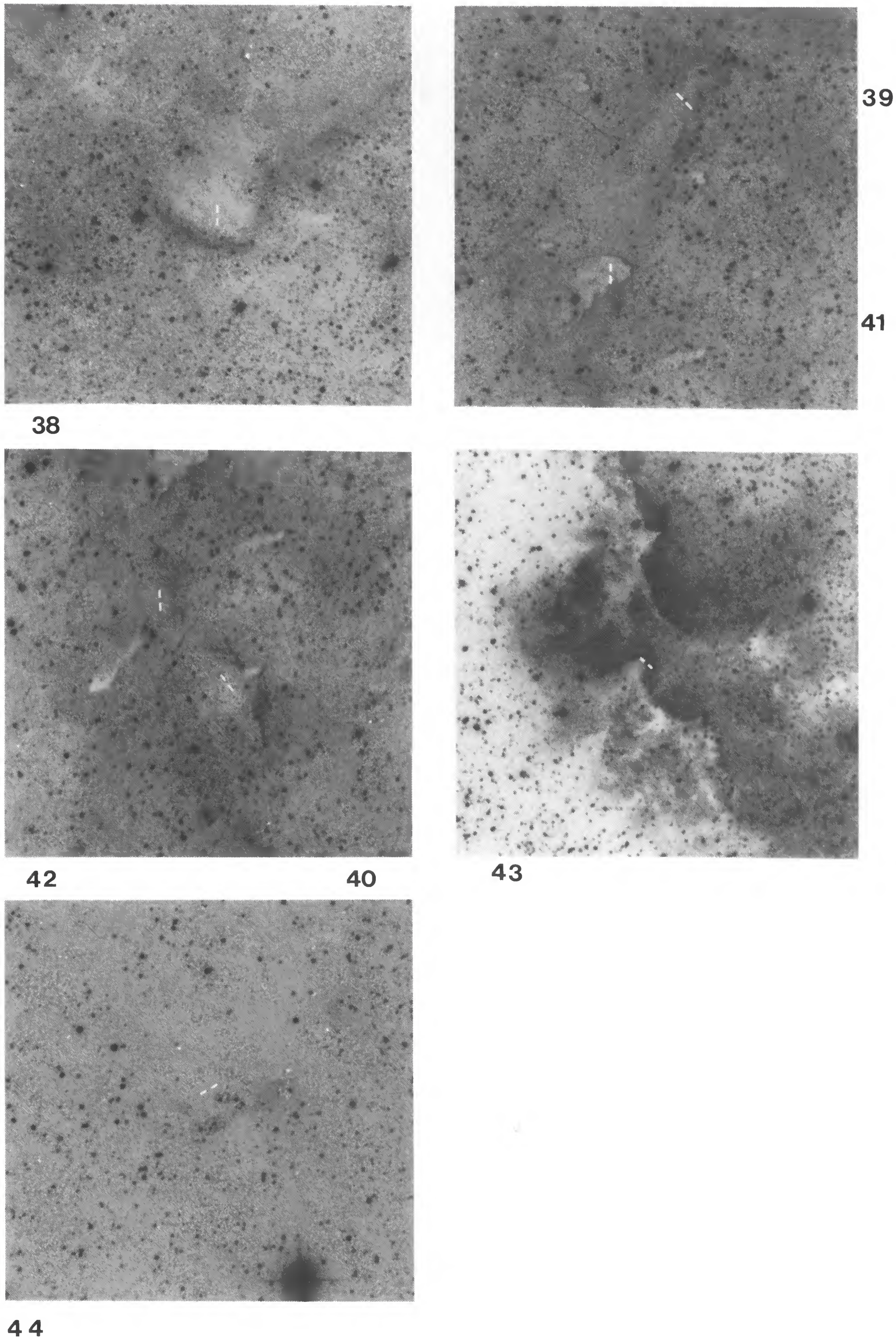

FIG. 1—*Continued*

SUGITANI et al. (*see* 77, 60)

TABLE 2

BRIGHT-RIMMED CLOUDS ASSOCIATED WITH *IRAS* POINT SOURCES

Cloud Number (1)	HII Region (2)	Rim Type (3)	*l* (pc) (4)	*w* (pc) (5)	α (1950) (6)	δ (1950) (7)	*IRAS* Source (8)
1	S171	B	0.31	0.60	23h56m53.3s	67°06'57"	23568+6706
2	(NGC7822)	A	0.46	0.86	0h01m23.0s	68°17'59"	00013+6817
3		C	0.39	0.16	0h02m47.9s	67°00'57"	00027+6700
4	S185	B	0.19	0.17	0h56m00.7s	60°37'21"	00560+6037
5	S190	B	1.33	1.40	2h25m14.5s	61°20'10"	02252+6120
6	(IC1805)	A	0.25	0.70	2h30m57.7s	60°34'41"	02309+6034
7		B	2.11	3.33	2h31m01.7s	61°33'40"	02310+6133
8		A	0.63	1.33	2h31m48.1s	61°06'32"	02318+6106
9		A	0.21	0.67	2h32m37.3s	61°10'34"	02326+6110
10	S199	A	0.46	1.16	2h44m23.9s	60°12'06"	02443+6012
11	(IC1848)	A	0.53	1.05	2h47m37.4s	59°50'54"	02476+5950
12		B	1.23	1.05	2h51m08.3s	60°23'35"	02511+6023
13		B	2.04	1.93	2h57m03.6s	60°28'29"	02570+6028
14		A	0.98	2.91	2h57m35.6s	60°17'22"	02575+6017
15	S236 (IC410)	B	0.82	1.44	5h20m13.3s	33°09'08"	05202+3309
16	S276	A	0.59	1.26	5h17m21.9s	-5°55'05"	05173-0555
17	S264	A	0.41	1.70	5h28m40.2s	12°03'13"	05286+1203
18	(λ Ori)	A	0.37	1.40	5h41m45.3s	9°07'40"	05417+0907
19	S277	A	0.18	0.41	5h32m00.4s	-3°00'12"	05320-0300
20	(IC434)	C	0.70	0.20	5h35m33.2s	-1°46'50"	05355-0146
21		A	0.09	0.22	5h37m11.8s	-3°38'46"	05371-0338
22	S281	B	0.62	0.37	5h35m58.5s	-5°15'48"	05359-0515
23	S249	A	0.74	1.77	6h19m56.5s	23°11'32"	06199+2311
24	S275 (NGC2244)	B	1.02	0.58	6h32m16.5s	4°27'40"	06322+0427
25	S273 (NGC2264)	B	0.65	1.22	6h38m17.6s	10°17'54"	06382+1017
26	S296	A	0.15	0.38	7h01m26.8s	-11°41'17"	07014-1141
27	(CMa OB1)	A	0.38	0.93	7h01m37.9s	-11°18'48"	07016-1118
28		A	0.32	0.76	7h02m21.4s	-10°17'25"	07023-1017
29		A	0.38	1.02	7h02m32.5s	-12°04'51"	07025-1204
30	S49	B	1.63	2.64	18h15m55.0s	-13°46'09"	18159-1346
31	S117 (NGC7000)	A	0.46	1.39	20h48m57.5s	44°10'43"	20489+4410
32	S131	A	0.17	0.69	21h30m52.7s	57°10'49"	21308+5710
33	(IC1396)	A	0.14	0.30	21h31m41.1s	57°16'13"	21316+5716
34		A	0.42	0.73	21h32m02.5s	57°50'06"	21320+5750
35		A	0.35	1.32	21h34m35.8s	58°18'10"	21345+5818
36		(AorC)	···	0.97	21h34m40.1s	57°14'05"	21346+5714
37	S131	C	0.65	0.19	21h38m53.2s	56°22'18"	21388+5622
38	(IC1396)	B	0.76	1.11	21h39m10.3s	58°02'29"	21391+5802
39		B	1.01	0.60	21h44m30.8s	57°12'29"	21445+5712
40		A	0.25	0.62	21h44m38.0s	56°55'05"	21446+5655
41		B	0.72	0.60	21h44m52.8s	57°04'46"	21448+5704
42		A	0.25	0.53	21h45m00.1s	56°58'30"	21450+5658
43	S142 (NGC7380)	B	0.36	1.55	22h45m48.5s	57°46'59"	22458+5746
44	S145	A	0.36	1.30	22h27m12.2s	63°58'21"	22272+6358A

COL. (1).—Cloud number.
COL. (2).—H II region where the bright-rimmed cloud was selected.
COL. (3).—Morphological type of the bright rim (see § 3.1).
COLS. (4)–(5).—Length and width of the bright rim.
COLS. (6)–(7).—1950 coordinates which are quoted from the positions in the *IRAS* Point Source Catalog.
COL. (8).—*IRAS* point source associated with the bright-rimmed cloud.

TABLE 3

PROPERTIES OF *IRAS* POINT SOURCES

Number (1)	*IRAS* Source (2)	12 μm (3)	25 μm (4)	60 μm (5)	100 μm (6)	CC (7)	Type (8)	L_{IR} ($L_{\odot}$) (9)	Outflow/HH (10)	Ref. (11)
1	23568+6706	5.80:	9.75	184.04	840.85	ECCA	II	750		
2	00013+6817	1.76	4.21	11.44	105.30 L	AACG	I	(33)		
3	00027+6700	0.82:	1.48	19.92	73.91 L	DCA....	II	(38)		
4	00560+6037	1.93	2.52	43.12	74.32	BBCA	II	5.2		
5	02252+6120	9.81	55.98	239.51 L	638.82 L	AAAA	III	(1100)	IC1805-west	1
6	02309+6034	0.59:	0.96	9.59:	29.53	GCCB	II	160		
7	02310+6133	0.92	2.44	51.51	189.68:	GDCB	II	910	(a)	
8	02318+6106	0.60	1.04	15.12:	71.94:	DDCC	II	330		
9	02326+6110	0.32:	0.69	5.81	37.48 L	FFBB	II	(61)		
10	02443+6012	0.71	1.02	3.44 L	102.86 L	CB...C	III	(30)		
11	02476+5950	0.27 L	0.33	2.05	12.45	GCCB	II	53		
12	02511+6023	1.31	2.91	34.47	110.47	CBAA	II	580	(a)	
13	02570+6028	4.82	8.13	78.34	231.45	BBAA	II	1300	(a)	
14	02575+6017	19.91	211.98	767.93	1083.15	AAAA	I	9800	AFGL4029	2
15	05202+3309	0.51	0.95	13.41 L	62.02 L	CBEF	III	(81)		
16	05173-0555	0.25 L	3.02	27.15	61.34:	GAAC	I	16	L1634/RNO40	1, 3
17	05286+1203	0.78	1.91	9.35:	70.37	CCEF	I	19		
18	05417+0907	0.28:	2.92	25.60	74.74	DAAB	I	18	B35	4
19	05320-0300	0.25 L	0.35	7.21:	25.00	HCEA	II	5.3		
20	05355-0146	0.38	1.40	13.32	42.09	EBBA	I	9.8	Ori I-2	5
21	05371-0338	0.48:	0.84	15.10:	69.12 L	FBDA	II	(6.3)		
22	05359-0515	1.44	1.95	18.85:	97.56 L	CCDA	II	(11)		
23	06199+2311	0.50	1.42	6.58	22.74 L	CAAH	I	(55)		
24	06322+0427	0.37 L	0.75	10.20	73.98 L	FDB...	II	(51)		
25	06382+1017	1.28	7.91	43.45	86.66	BAAA	I	100	HH124[b]	6
26	07014-1141	0.61	1.01	11.85	23.50:	CCBE	II	57		
27	07016-1118	1.86	1.44:	32.03:	144.62 L	FFEK	II	(110)		
28	07023-1017	1.15	1.77	50.23:	134.25 L	CCBB	II	(170)		
29	07025-1204	0.26	1.36	10.12	33.23:	CAAA	I	64		
30	18159-1346	5.97	19.30:	169.86 L	5317.44 L	BBE...	III	(590)		
31	20489+4410	3.56	10.48	49.62	158.64 L	BABH	I	(160)		
32	21308+5710	0.68	1.18	10.23	62.94	CCDA	II	43		
33	21316+5716	0.99	1.36	33.46 L	73.10 L	DBBC	III	(6.4)		
34	21320+5750	0.77	2.40	11.91 L	37.25 L	BAAB	III	(8.6)		
35	21345+5818	0.58	0.60:	8.15:	80.34 L	EFBF	II	(13)		
36	21346+5714	0.74	1.51	28.01:	164.75:	DAAC	II	110		
37	21388+5622	2.44	17.44	52.67	74.84	AAAA	I	110	GN21.38.9	7
38	21391+5802	0.56:	8.90	144.62	425.20	DAAA	I	340	IC1396-north	5
39	21445+5712	3.01	11.34	34.75	86.75	AAAA	I	96	IC1396-east	1
40	21446+5655	0.38:	0.63	20.42 L	41.48:	FCBA	III	(23)		
41	21448+5704	0.30 L	0.83	3.98	100.21 L	NDBC	I	(6.4)		
42	21450+5658	0.76	1.19	15.19	62.76:	CCBC	II	47		
43	22458+5746	5.83	30.31	431.31 L	384.32 L	AABF	III	(1000)		
44	22272+6358A	0.25 L	18.01	378.36	726.92	JAAA	I	1000	L1206	5

COL. (1).—Identification number.

COL. (2).—Name of the *IRAS* point source.

COLS. (3)–(6).—*IRAS* fluxes at the four wavelengths, where "L" and ":" denote upper limit and "moderate" quality, respectively.

COL. (7).—Correlation coefficients of the *IRAS* point source.

COL. (8).—Classification of the *IRAS* point source according to its colors (see § 3.2).

COL. (9).—Luminosity of the *IRAS* point source, where the parentheses denote the *IRAS* source with fluxes of upper limits at 60 μm and/or 100 μm.

COLS. (10)–(11).—Known molecular outflow or HH object associated with the *IRAS* point source and its reference.

[a] Associated with a high-velocity CO wing (see § 3.2).

[b] No detection of molecular outflow.

REFERENCES.—(1) Fukui 1989; (2) Snell et al. 1988; (3) Cohen 1980; (4) Myers et al. 1988; (5) Sugitani et al. 1989; (6) Walsh, Ogura, & Reipurth 1991; (7) Duvert et al. 1990.

Bright-rimmed clouds appear to be composed of a dense head/front part and a less dense tail. Star formation should occur in the dense head part. We made a rough estimate of radii for the head part clouds based on the sizes measured above. Assuming a round shape of the head part cloud, its "radius" R was estimated as follows: (1) type A, $R = l/2$; (2) type B, $R = w/4$; and (3) type C: $R = w/2$. All the radii estimated are $\lesssim$0.9 pc and most of them are $\lesssim$0.5 pc as shown in Figure 3. The ranges of types A, B, and C are 0.04–0.5, 0.04–0.9, and 0.08–0.1 pc, respectively. We note that these sizes of the bright-rimmed clouds are similar to the radii of the Bok globules (Bok & Cordwell 1973; Bok 1977; Martin & Barrett 1978).

The densities and masses are known for only a limited number of the bright-rimmed clouds which have been observed in molecular lines. We estimated the masses contained in the head part clouds $M'_{\rm cloud}$ by $M'_{\rm cloud} = 4/3\pi R^3 mn$, where R is the radius defined above, m the hydrogen molecular weight, and n the assumed number density of 3×10^4 H_2 which is the average density of the three bright-rimmed globules, Ori I-2, IC1396-north, and L1206, derived from the ^{13}CO observations (Sugitani et al. 1989). Because of the uncertainty in the radius determination (a few 10%), the masses $M'_{\rm cloud}$ are considered uncertain by a factor of a few. The range of the $M'_{\rm cloud}$ is $\sim$1–1900 $M_{\odot}$, with most of them less than 100 $M_{\odot}$. The average $M'_{\rm cloud}$ of the three rim types are as follows: type A: 44$M_{\odot}$ (25), type B:

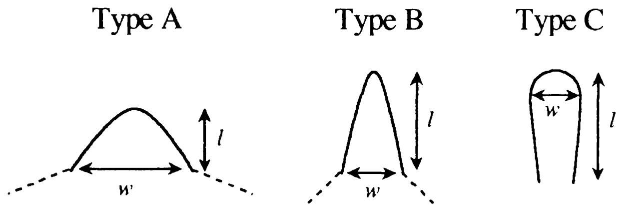

FIG. 2.—Classification of the rim shape and definition of the rim size

$86 M_\odot$ (13, except for the two highest mass clouds), and type C: 2.6 $M_\odot$ (3). These values are similar to those of the Bok globules (Bok & Cordwell 1973, Bok 1977; Martin & Barrett 1978).

3.2. *Associated IRAS Point Sources*

Figure 4 shows the 12/25/60 μm color–color diagram for the 44 *IRAS* sources, with the exception of eight sources not detected at 60 μm. On the color-color diagram, the *IRAS* sources are divided into two types as in Beichman (1983). One type includes those sources with a distribution similar to that of the core sources, which are considered to be newly formed or still-forming stars embedded in their parental clouds. The other type are sources with a distribution similar to that of the hot cirrus sources, which are considered to be compact structures of the cirrus. Here we refer to the former as type I and to the latter as type II. The numbers of type I and type II sources are 15 and 21, respectively. With an average value of 99.6%, the correlation coefficients at 25 μm of the type I sources are good, *D* or better (see col. [7] of Table 3). The coefficients of the type II sources are rather good, with an average value of 97.7% at 25 μm. Although the type II sources have a distribution similar to that of the hot cirrus sources on the color–color diagram, the type II sources have better correlation coefficients than the hot cirrus sources (Beichman 1983). The eight sources which are not detected at 60 μm (six of them are also not detected at 100 μm) have again high correlation coefficients, an average value of 99.3% at 25 μm. We refer to these eight sources as type III.

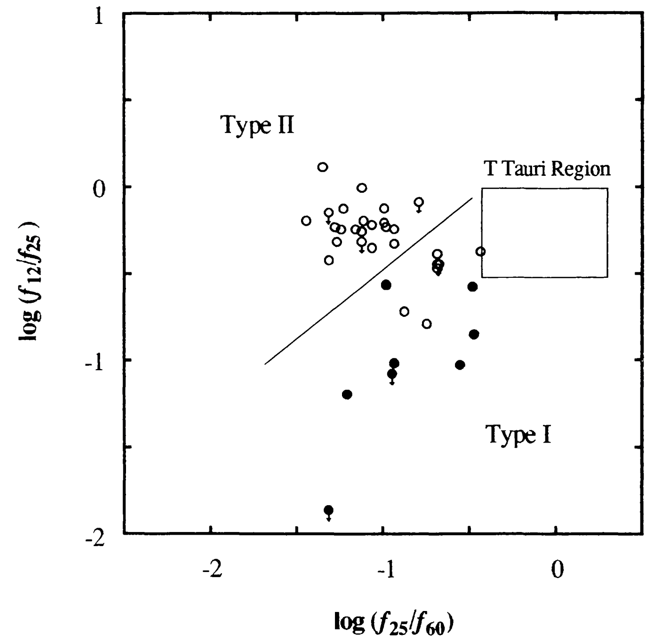

FIG. 4.—12/25/60 μm color-color diagram of the *IRAS* point sources. Filled circles denote the *IRAS* sources associated with molecular outflows. Down arrows indicate upper limits at 12 μm.

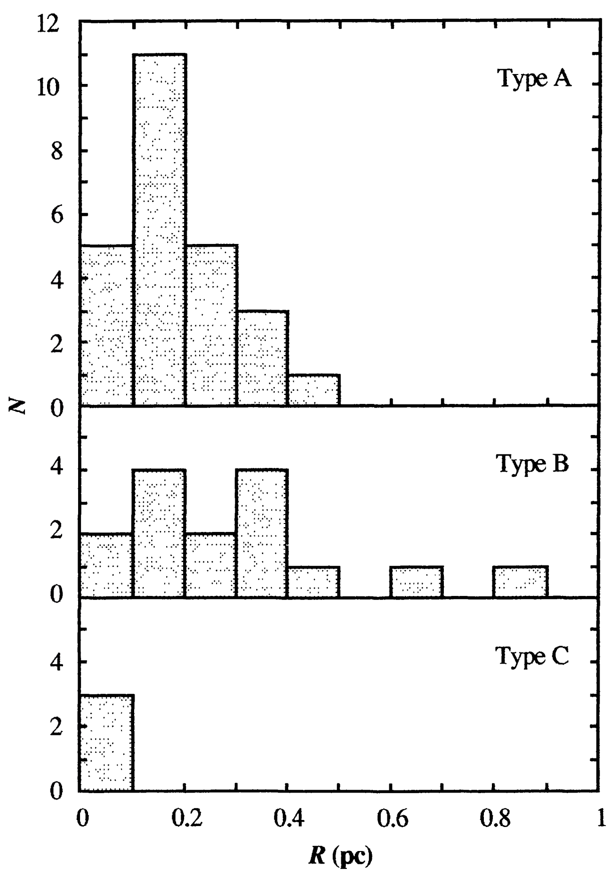

FIG. 3.—Distribution of the cloud radii estimated from the rim sizes (see text), except for No. 36.

We derived the luminosities $L_{\rm IR}$ of the *IRAS* sources (Table 3), following Myers et al. (1987). To accurately examine the luminosity function of the *IRAS* sources, we use only the 24 *IRAS* sources whose fluxes were detected at least in the three bands centered at 25, 60, and 100 μm. The distribution of the $L_{\rm IR}$ for the 24 sources (except for source No. 36) is shown in Figure 5, which indicates that the $L_{\rm IR}$ ranges from 5 to $10^4 L_\odot$. The type A clouds peak at $\sim 100 L_\odot$ in the luminosity distribution of the *IRAS* sources, whereas the type B clouds peak at $\sim 1000 L_\odot$. The logarithmic averages of the *IRAS* luminosities for the types A, B, and C clouds are 1.9 (13), 2.4 (8), and 1.5 (2), respectively. The average of the 24 sources is ~2.0, which is about two orders of magnitude larger than that of the *IRAS* sources associated with dark globules, ~0.46 (Sugitani et al. 1990) or dense cores in molecular cloud complexes, ~0.12 (Beichman et al. 1986).

Information on molecular outflows and HH objects associated with the *IRAS* sources is also shown in Table 3. Not all sources have been checked for outflows. At present, nine of the 44 bright-rimmed clouds are known to have outflows asso-

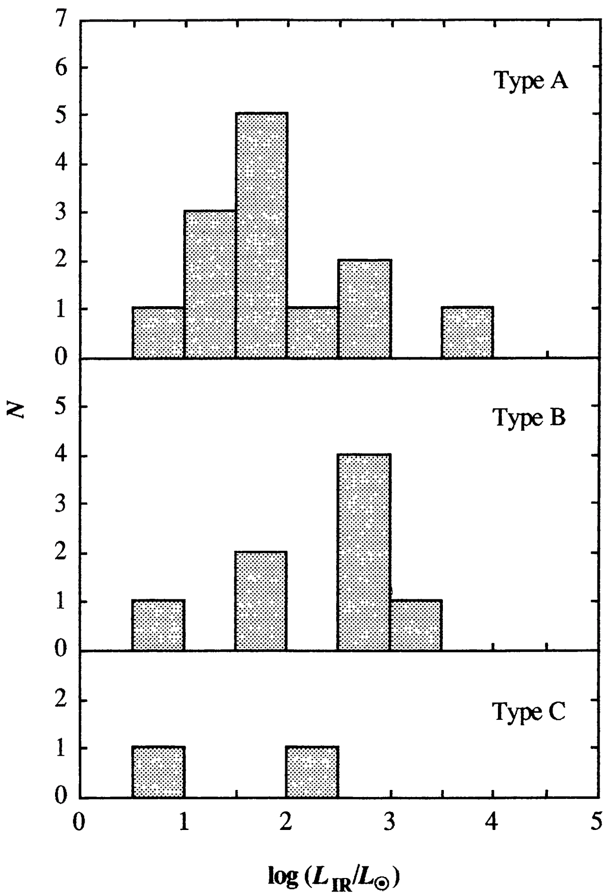

FIG. 5.—Distribution of the luminosities of the *IRAS* point sources.

ciated with the *IRAS* sources (Myers et al 1988; Snell et al. 1988; Sugitani et al. 1989; Fukui 1989; Duvert et al. 1990). Eight of the *IRAS* sources are type I, and the other is type III. The present detection rate of outflows for all the 44 *IRAS* sources is rather high, 20% (9/44). Recently, we searched some of the type II sources for outflows with the KOSMA 3 m telescope, and confirmed CO(J = 2–1) wing emissions associated with the clouds of sources 7, 12, and 13.

4. DISCUSSIONS

4.1. *Properties of IRAS Sources*

The 44 *IRAS* sources selected here are considered to be good candidates for embedded young stellar objects or T Tauri stars. All the *IRAS* sources are located toward the regions of high visual extinction on the PSS prints, which is similar to the situation of *IRAS* sources associated with dark globules or cloud cores in molecular cloud complexes.

The type I sources are most likely young stellar objects embedded in molecular cloud cores. Part of the type I sources have so far been searched for molecular outflows and with a detection rate of 53% they are really young stellar objects.

The color-color plots suggest that the type II sources have warm 12/25 μm color indexes like the hot cirrus sources. However, the bright-rimmed clouds are located toward H II regions and can, therefore, be strongly contaminated by their associated and extended emission, particularly at longer wavelengths of the *IRAS*. For one *IRAS* source in L1686, Beichman et al. (1986) mentioned that the extended emission confuses the measurement of the long-wavelength properties. It is, therefore, possible that the 25/60 μm color indexes become smaller than their actual values due to the excess emission at 60 μm from the H II region. If this is the case for the type II sources, most of them should actually have spectral energy distributions similar to those of T Tauri stars. Although the *IRAS* sources in B335 and Cep C have 12/25/60 μm color-color indexes similar to the hot cirrus sources, they are associated with molecular outflows (Goldsmith et al. 1984; Fukui 1989). Three type II sources, i.e., sources 7, 12, and 13, may be associated with molecular outflows. Correlation coefficients of the type II sources at 25 μm are good, which may support that most of the type II sources are young stellar objects with warmer 12/25 μm color indexes than those of the core sources and are older than the core sources (Fukui et al. 1989).

Type III sources were not detected at 60 μm. The reason for the nondetection may be similar to the case for the type II sources. One of them, *IRAS* 02252+6120, is associated with an outflow (IC 1805-west; Fukui 1989) and an emission line star (Ogura 1989), although its fluxes at 60 and 100 μm represent upper limits.

4.2. *Star Formation in the Bright-rimmed Clouds*

Most of the *IRAS* sources associated with the bright-rimmed clouds have L_{IR} from $\sim$10 to 10^3 $L_{\odot}$ (Fig. 5). Generally the mass determination of a young stellar object is difficult, but this luminosity range may roughly correspond to intermediate masses of stars, something like $\sim$2–6 $M_{\odot}$, suggesting that intermediate-mass stars are mainly formed in the bright-rimmed clouds. The luminosity detection limit of the *IRAS* sources in this survey may be $\sim$10 $L_{\odot}$, judging from the survey results. It is likely that we missed some quite bright-rimmed clouds associated with low-mass young stellar objects.

We have calculated *normalized IRAS* luminosities per unit cloud mass, L_{IR}/M'_{cloud} following Sugitani et al. (1989). The result shows that the L_{IR}/M'_{cloud} are between 0.1 and 10^2 $L_{\odot}/M_{\odot}$ (Fig. 6). The logarithmic averages for the 24 clouds with type A, B, and C rims (except for No. 36 cloud) are 0.49 (13), 1.0 (8), and 1.0 (2), respectively. The logarithmic average of the 23 clouds is $\sim$0.7 ($\approx$5 $L_{\odot}/M_{\odot}$), which is much larger than typical values for isolated dark Bok globules, $\sim$0.1 $L_{\odot}/M_{\odot}$ (Sugitani et al. 1989) and for the dense cores, $\sim$1/30 $L_{\odot}/M_{\odot}$ ($\sim$1 $L_{\odot}$: Beichman et al. 1986; $\sim$30 $M_{\odot}$: Myers, Linke, & Benson 1983). For the latter case, the cloud masses were derived from ^{18}CO observations and have a similar mass range. The assumption of constant cloud density and a radius R estimated from the l and w may be in doubt. Consequently, L_{IR}/M'_{cloud} might have large errors (a factor of a few or more). Nevertheless, since the differences are very large, about two orders of magnitude, we consider that the luminosity-to-mass ratios are large in the bright-rimmed clouds. If we adopt a relationship between stellar luminosity and mass of $L \propto M^{3-4}$, the difference of about two orders of magnitude can be explained by formation of 3–4 times more massive stars in the bright-rimmed clouds.

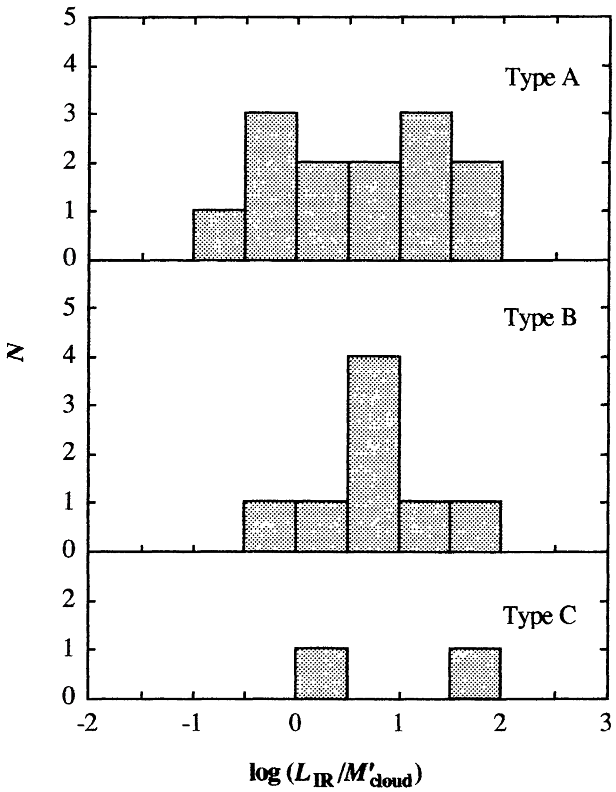

FIG. 6.—Distribution of the luminosity to mass ratios of the bright-rimmed clouds. The masses were estimated from the cloud radii assuming a constant density (see text).

4.3. *Characteristics of Star Formation by Radiation-driven Implosions*

The radii of the bright-rimmed clouds are mostly less than 0.5 pc. The accretion shock velocity in the bright-rimmed clouds is ~ 10 km s^{-1} (Bertoldi 1989), which suggests an implosion time scale of $\lesssim 10^5$ yr. *IRAS* point sources embedded in molecular cloud cores are considered to be $\sim 10^5$ yr-old (e.g., Beichman et al. 1986). The average extent of these 18 H II regions is $\sim$48 pc, and with an adopted expansion velocity of a H II region of ~ 10 km s^{-1}, we obtain a dynamical age of $\sim$2–3×10^6 yr, which is much larger than the implosion time scale or the age of the *IRAS* source. One should, therefore, expect to find signs of star formation triggered by the radiation-driven implosions in the bright-rimmed clouds.

The number of the bright-rimmed clouds with *IRAS* sources per H II region varies from 1 to 11 in this work. The average number per H II region is $\sim$2.4, which may be a lower limit, because we picked up only the bright-rimmed clouds located on the near sides of the H II regions. This value should then be doubled, i.e., $\sim$5.

We can thus roughly estimate a total number of stars formed during a lifetime of a H II region to be ~ 100, if we assume that five stars are formed in five clouds during 10^5 yr and that star formation lasts steadily during 2×10^6 yr. A study of Hα emission line stars in the region of IC 1396 suggests, in accordance with our estimate, that $\sim$300 emission-line stars probably associated with IC 1396 are mostly pre-main-sequence stars with masses from 1.5 $M_\odot$ to 3 $M_\odot$ (Kun & Pásztor 1990).

We found the bright-rimmed clouds with *IRAS* sources in 18 H II regions. Ten of the 18 H II regions are within 1 kpc. This value of 10 should be increased by a factor of 1.5, because the PSS prints cover only two-thirds of the whole sky. If 100 stars with masses of 2 $M_\odot$ are formed during the life time of a H II region, i.e., 1500 stars per 2×10^6 yr within 1 kpc, and if such star formation is over the entire Galaxy, we can expect a surface star formation efficiency of $\sim 5 \times 10^{-4}$ $M_\odot$ kpc^{-2} yr^{-1}. Adopting a radius of ~ 10 kpc and an overall star formation efficiency for the Galaxy of ~ 3 $M_\odot$ yr^{-1}, we obtain a rate of $\sim 10^{-2}$ $M_\odot$ kpc^{-2} yr^{-1}, suggesting that $\sim$5% by mass of the stars in the Galaxy are formed through the implosion process. Stars with masses between 1.5 and 6 $M_\odot$ have 30% of the total mass in the IMF (Miller & Scalo 1979). If we assume that the IMF is universal in the Galaxy, this percentage of $\sim$5 corresponds to $\sim$15% of the intermediate-mass stars. Most of the values used for the estimate may be lower limits and the percentage of $\sim$15 should be considerably increased. Therefore, we conclude that star formation by the implosions can make a great contribution to the formation of intermediate-mass stars.

5. SUMMARY

We have surveyed small bright-rimmed clouds associated with *IRAS* point sources with the aim of detecting candidates of star formation induced by the radiation-driven implosions. The Palomar Sky Survey prints and *IRAS* Point Source Catalog were used for this survey. The surveyed regions are mainly around H II regions of Sharpless (1959) with extents of $\sim$60′ or larger. The main findings of this survey are as follows:

1. Forty-four bright-rimmed clouds with *IRAS* point sources were selected from the 18 H II regions of Table 1.
2. Nine of the 44 bright-rimmed clouds are associated with molecular outflows. Two clouds out of the 44 clouds are associated with HH objects, including one cloud with an outflow.
3. Most of the bright-rimmed clouds have small radii of $\lesssim$0.5 pc, which are similar to those of the dark globules or to the dense cores in dark cloud complexes. The clouds also appear to have a similar mass range, mostly $\lesssim$100 $M_\odot$.
4. The associated *IRAS* sources have luminosities of $\sim$10–10^4 $L_\odot$, which are on the average by about two orders of magnitude larger than those of the *IRAS* sources associated with the dark globules or the dense cores. The L_{IR}/M'_{cloud} ratio is also larger in the bright-rimmed clouds by about two orders of magnitude. These two results suggest that intermediate-mass stars are mainly formed in the bright-rimmed clouds.
5. Stars formed through the radiation-driven implosions are expected to contribute $\sim$5% of the total stellar mass in the Galaxy. A significant number of intermediate-mass stars may be formed in bright-rimmed clouds around H II regions.

We would particularly like to thank Gisbert Winnewisser and Juergen Stutzki for helpful comments and support. We would also like to thank Akira Mizuno for preparing photographs. This work was financially supported in part by the Grant-in-Aid for Scientific Research (A) No. 6342003 and 6242002, and the Grant-in-Aid for Specially Promoted Research No. 01065002 in the Ministry of Education, Culture, and Science of Japan, and in part by the Deutsche Forschungsgemeinschaft through SFB301.

REFERENCES

Bally, J., & Scoville, N. Z. 1980, ApJ, 239, 121
Bedijn, P. J., Tenorio-Tagle, G. 1984, A & A, 135, 81
Beichman, C. A. 1983, in Light on Dark Matter, ed. F. P. Israel (Dordrecht: Reidel), p. 279
Beichman, C. A., Myers, P. C., Emerson, J. P., Harris, S., Mathieu, R., Benson, P. J., & Jennings, R. E. 1986, ApJ, 307, 337
Bertoldi, F. 1989, ApJ, 346, 735
Bertoldi, F., & Mckee, C. F. 1990, ApJ, 354, 529
Blaauw, A., 1964, ARA&A, 2, 213
Bok, B. J. 1977, PASP, 89, 597
Bok, B. J., & Cordwell, C. S. 1973, in Molecules in the Galactic Environment, ed. M. A. Gordon & L. E. Snyder (New York: Wiley-Interscience)
Bok, B. J., Cordwell, C. S., & Cromwell, R. H. 1971, in Dark Nebulae, Globules, and Protostars, ed. B. T. Lynds (Tucson: University of Arizona Press), p. 33
Claria, J. J. 1974, A&A, 37, 229
Cohen, M. 1980, ApJ, 85, 29
Crampton, D., & Fisher, W. A. 1974, Pub. Dom. Ap. Obs., 14, No 12
Duvert, G., Cernicharo, J., Bachiller, R., & Gómez-González, J. 1990, A&A, 233, 190
Elmegreen, B. G. 1988, ApJ, 326, 616
Fukui, Y. 1989, in Low-Mass Star Formation and Pre–Main-Sequence Objects, ed. B. Reipurth (Garching: ESO), p. 95
Fukui, Y., Iwata, T., Takaba, H., Mizuno, A., Ogawa, H., Kawabata, K., & Sugitani, K. 1989, Nature, 342, 171
Fukui, Y., Sugitani, K., Takaba, H., Iwata, T., Mizuno, A., Ogawa, H., & Kawabata, K. 1986, ApJ, 311, L87
Georgelin, Y. M., & Georgelin, Y. P. 1976, A&A, 49, 57
Goldsmith, P. F., Snell, R. L., Hemeon-Heyer, M., & Langer, W. D. 1984, ApJ, 286, 599
Hardie, R. H., Seyfert, C. K., & Gulledge, I. S. 1960, ApJ, 132, 361
Humphreys, R. M. 1978, ApJS, 38, 309
IRAS Catalogs and Atlases, Explanatory Supplement. 1984, ed. C. A. Beichman, G. Neugebauer, H. J. Habing, P. E. Clegg, & T. J. Chester (Washington, DC: US GPO)
Ishida, K. 1970, PASP, 22, 277
King, D. J. 1987, MNRAS, 226, 473
Klein, R. I., Sandford, M. T., & Whitaker, R. W. 1980, Space Sci. Rev., 27, 275
———, 1985, in Protostars and Planets II, ed. D. C. Black & M. S. Matthews (Tucson: University of Arizona Press), p. 340
Kun, M., & Pásztor, L. 1990, Ap. Space Sci., 174, 13
LaRosa, T. N. 1983, ApJ, 274, 815
MacConnell, D. J. 1968, ApJS, 16, 275
Martin, R. N., & Barrett, A. H. 1978, ApJS, 36, 1
Matthews, H. E. 1979, A&A, 75, 345
Miller, G. E., & Scalo, J. 1979, ApJS, 41, 513
Murdin, P., & Penston, M. V. 1977, MNRAS, 181, 657
Myers, P. C., Fuller, G. A., Mathieu, R. D., Beichman, C. A., Benson, P. J., Schild, R. E., & Emerson, J. P. 1987, ApJ, 319, 340
Myers, P. C., Hyer, M., Snell, R. L., & Goldsmith, P. F. 1988, ApJ, 324, 907
Myers, P. C., Linke, R. A., & Benson, P. J. 1983, ApJ, 264, 517
Ogura, K. 1989, private communication
Ogura, K., & Ishida, K. 1981, PASJ, 33, 149
Olberg, M., Reipurth, B., & Booth, R. S. 1989, in The Physics and Chemistry of Interstellar Molecular Clouds, ed. G. Winnewisser & J. T. Armstrong (Heidelberg: Springer-Verlag), p. 120
Osterbrock, D. E. 1957, ApJ, 117, 183
Reipurth, B., 1983, A&A, 117, 183
Reipurth, B., & Gee, G. 1986, A&A, 166, 148
Reynolds, R. J., & Ogden, P. M. 1979, ApJ, 229, 942
Sandford, M. T., II, Whitaker, R. W., & Klein, R. I. 1982, ApJ, 260, 183
———. 1984, ApJ, 282, 178
Savage, B. D., Bohlin, R. C., Drake, J. F., & Budich, W. 1977, ApJ, 216, 291
Sharpless, S. 1959, ApJS, 4, 257
Snell, R. L., Huang, Y.-L., Dickman, R. L., & Claussen, M. J. 1988, ApJ, 325, 853
Stutzki, J., & Güsten, R. 1990, ApJ, 356, 513
Sugitani, K., Fukui, Y., Mizuno, A., & Ohashi, N. 1989, ApJ, 342, L87
Turner, D. G. 1976, ApJ, 210, 65
Walsh, J. R., Ogura, K., & Reipurth, B. 1991, in preparation